Formation of Multiple-Flux-Quantum Vortices in Mesoscopic Superconductors from Simulations of Calorimetric, Magnetic, and Transport Properties

Ben Xu,[1] M. V. Milošević,[1] Shi-Hsin Lin,[2,1] F. M. Peeters,[1,*] and B. Jankó[2]

[1]*Departement Fysica, Universiteit Antwerpen, Groenenborgerlaan 171, B-2020 Antwerpen, Belgium*
[2]*Department of Physics, University of Notre Dame, Notre Dame, Indiana 46556, USA*

Because of strong flux confinement in mesoscopic superconductors, a ''giant'' vortex may appear in the ground state of the system in an applied magnetic field. This multiquanta vortex can then split into individual vortices (and vice versa) as a function of, e.g., applied current, magnetic field, or temperature. Here we show that such transitions can be identified by calorimetry, as the formation or splitting of a giant vortex results in a clear jump in measured heat capacity versus external drive. We attribute this phenomenon to an abrupt change in the density of states of the quasiparticle excitations in the vortex core(s), and further link it to a sharp change of the magnetic susceptibility at the transition—proving that the formation of a giant vortex can also be detected by magnetometry.

The influence of quantum confinement on superconducting condensates is one of the prominent research directions in low-temperature physics of the last decade. Vortex matter in conventional but mesoscopically tailored superconducting samples has especially generated tremendous interest and activity in the wide scientific community. Namely, vortices are of direct relevance to cold gases and Bose-Einstein condensates [1]; interaction of vortices with artificial pinning sites has analogues in colloidal systems and molecular crystals [2]; the inhomogeneous field of vortices can confine spin textures in a nearby magnetic semiconductor—thus manipulation of vortex states can be useful in spintronics [3]; the ''ratchet'' dynamics of vortices in asymmetric pinning profiles is directly related to biological microdevices that separate particles by converting random motion into directed motion [4].

One of the most puzzling questions in the area of vortex matter in submicron samples is the distinction between two allotropies of a vortex state—a ''giant'' vortex, where all vortices merge into a single singularity, and a multivortex, where all vortices can be individually resolved. In type-II superconductors, transitions between the latter two states are of second order, following the increasing lateral compression by, e.g., increasing screening currents in increasing magnetic field [5], or increasing temperature which makes the sample effectively smaller in terms of the superconducting length scales. Even in numerical calculations, it is very difficult to pinpoint the exact value of parameters for the giant-to-multi crossover, as the order parameter is severely suppressed between vortices in close proximity. It is therefore no surprise that imaging experiments could not verify the existence of a giant vortex beyond reasonable doubt [6]. Several years ago, Kanda *et al.* conveyed a clever transport measurement, where distinction between giant and multivortex states was made by symmetry matching between the vortex configuration and the location of

several tunnel junctions [7]. Although not always conclusive (e.g., if sample and vortex arrangement match in symmetry), this is the best known method to date for giant-vortex detection.

In this Letter, we present a universal method for the observation of formation and decay of multiquanta vortex states. Our theoretical simulations indicate that the experimentally measured heat capacity of a mesoscopic superconductor as a function of the magnetic field or temperature can unambiguously reveal such transitions. The underlying reason can be traced back to the behavior of the local density of states for quasiparticles, and we demonstrate a direct link between the heat capacity and the sample magnetization. With recent advances in calorimetry [8] and magnetometry [9] of submicron samples, our findings are of immediate relevance to current experimental efforts.

The Ginzburg-Landau (GL) formalism has been extensively used in the past to gain theoretical insight in the physics of mesoscopic superconductors. The core of the approach is the GL energy functional

$$\mathcal{G} = \int \left[-|\psi|^2 + \frac{1}{2}|\psi|^4 + \frac{1}{2}|(-i\nabla - \mathbf{A})\psi|^2 + \kappa^2(\mathbf{h} - \mathbf{H})^2 \right] dV, \tag{1}$$

describing the difference in Gibbs free energy between the superconducting (S) and normal (N) state in units of $\mathcal{G}_0 = H_c^2/8\pi$. Here κ denotes the GL parameter and determines screening of the applied magnetic field $\mathbf{H}$ from the given superconducting material. In Eq. (1) all distances are scaled by the coherence length ξ, the vector potential $\mathbf{A}$ by $c\hbar/2e\xi$, the magnetic field $\mathbf{h}$ by $H_{c2} = c\hbar/2e\xi^2 = \kappa\sqrt{2}H_c$, and the order parameter ψ by its equilibrium value in the absence of the magnetic field. The minimization of $\mathcal{G}$

　　　　　057002-1

is numerically equivalent to solving two coupled GL equations, and for details of this procedure we refer to Ref. [10]. Once a stable solution is found, we are able to calculate the specific heat of the superconducting state from the relation $C = -T\partial^2\mathcal{G}/\partial T^2$ [11], as a difference between the total heat capacity and that of the sample in the normal state, in units of $C_0 = H_c^2(0)V/(8\pi T_c)$. We start from the equilibrium states, increase or decrease the temperature of the system by $10^{-4}T_c$, and calculate numerically the second derivative. In what follows, we apply this method for a superconducting disk, a simple geometry already accessible both theoretically [5] and experimentally [6–9].

Figure 1 shows the energy of all the vortex states found in an aluminum superconducting disk of radius $R = 850$ nm and thickness $d = 100$ nm, at $T = 1.1$ K [we use $\xi(0) = 100$ nm, $\kappa = 1.2$, and $T_c = 1.38$ K [12]]. Because of the stronger interaction of the flux quanta with lateral boundaries for increased vorticity, all states in Fig. 1 with $L > 5$ are giant vortices. However, for $2 < L \le 5$ multivortex states can be found at lower magnetic field, which are compressed into a giant vortex at higher applied field. This is a gradual, second-order transition, and is therefore invisible in the free energy curves [5]. For clarity, we made a distinction between the multi- and giant vortex in Fig. 1 by dashed and solid lines, respectively. In what follows, we discuss the repercussions of the latter transition on the heat capacity of the sample.

Using attojoule calorimetry, Ong *et al.* [13] found that the heat capacity of mesoscopic disks is directly linked to the vorticity, exhibiting jumps as a function of the magnetic field—at transitions between vortex states. We argue here that the heat capacity depends not only on the number of vortices in the sample, but also on their configuration.
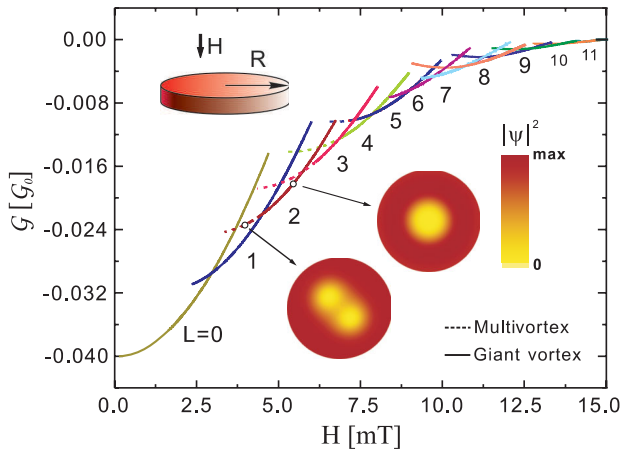

FIG. 1 (color online). The energy of different vortex states for an Al superconducting disk of radius $R = 850$ nm and thickness $d = 100$ nm, at $T = 0.8T_c$, for taken $\xi(0) = 100$ nm and $\kappa = 1.2$. Solid lines indicate giant-vortex states and dashed lines represent multivortex states. Insets show the density of the superconducting condensate for a $L = 2$ vortex state in multi and giant form.

Namely, the susceptibility of the sample to heating is linked to the kinetic energy of the Cooper pairs in and around the vortex core(s), and the changes in their trajectory upon the multi-to-giant vortex transition. In Fig. 2, we show the calculated heat capacity as a function of applied magnetic field for vortex states with vorticity 2 and 3, both exhibiting multi-to-giant vortex transition in Fig. 1. For both cases, the general trend of increasing heat capacity with field is interrupted exactly at the multi-to-giant vortex transition, where a sharp decrease of heat capacity is found.

In what follows, we show that the cause of the observed change in heat capacity during the merging of vortices is the changing local density of states (LDOS) for quasiparticle excitations inside the vortex cores. Actually, already from the early theoretical works (see Ref. [14]), we know that the bound state spectrum inside the vortex is also a function of momentum along the vortex line; as a result, the lowest bound state energy for winding number $L > 1$ is L times larger than that of winding number 1. Therefore, one expects that the low-energy states are pushed toward higher energies during merging of individual vortices into a giant vortex. To give a quantitative measure of this process, we first obtain the order parameter ψ and vector potential $\mathbf{A}$ of the equilibrium states from the GL calculation, which then serve as inputs for the microscopic Eilenberger equation

$$-i\hbar\mathbf{v}_F \cdot \nabla\hat{g}(\mathbf{r}, i\tilde{\varepsilon}_n) = \left[\begin{pmatrix} i\tilde{\varepsilon}_n & -\Delta(\mathbf{r}) \\ \Delta^\dagger(\mathbf{r}) & -i\tilde{\varepsilon}_n \end{pmatrix}, \hat{g}(\mathbf{r}, i\tilde{\varepsilon}_n)\right], \quad (2)$$

where $i\tilde{\varepsilon}_n(\mathbf{r}) = i\varepsilon_n(\mathbf{r}) + \mathbf{v}_F \cdot \frac{e}{c}\mathbf{A}(\mathbf{r})$, and $\hat{g} = \begin{pmatrix} ig & f \\ -f^\dagger & -ig \end{pmatrix}$ with normalization $\hat{g}(\mathbf{r}, i\tilde{\varepsilon}_n)\hat{g}(\mathbf{r}, i\tilde{\varepsilon}_n) = -\pi^2\hat{1}$. Equation (2) is further parametrized by $f = \frac{2a}{1+ab}$, $f^\dagger = \frac{2b}{1+ab}$, and $g = \frac{1-ab}{1+ab}$, where functions a and b now satisfy the independent nonlinear Ricatti equations [15]. In the next step, the LDOS is evaluated from

$$N(E, \mathbf{r}) = N_0 \int_0^{2\pi} \frac{d\theta}{2\pi} \rho(\theta) \operatorname{Re}\mathbf{g}(i\varepsilon_n \to E + i\eta, \mathbf{r}, \theta), \quad (3)$$
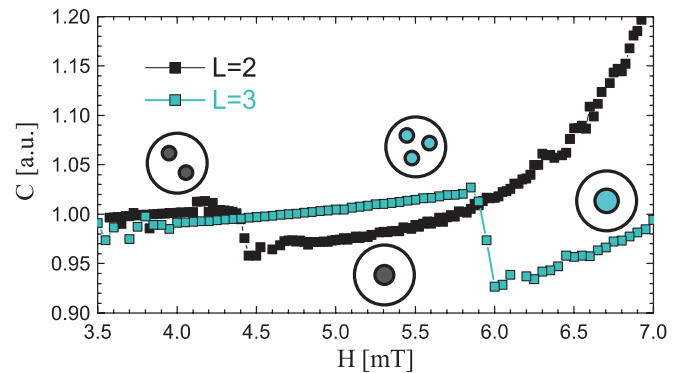

FIG. 2 (color online). The heat capacity as a function of magnetic field, for states with vorticity 2 and 3 of the sample considered in Fig. 1. The insets depict the vortex configuration before and after the multi-to-giant vortex transition.

where η (>0) is a small real constant. To obtain $\mathbf{g}(i\varepsilon_n \rightarrow E + i\eta, \mathbf{r}, \theta)$, we solve the Eilenberger equations for $\eta - iE$ instead of the Matsubara frequency ω_n. In order to find the LDOS, the above equations should be solved for a bundle of trajectories with different angle θ, running through the given point $\mathbf{r}$ and energy ε. In our calculation we consider only specular reflection for trajectories encountering the outer boundary of the sample.

Early theoretical works already considered LDOS of a single vortex [16]. Further, in Ref. [17] LDOS was calculated semiclassically for a multivortex vs the case of a giant vortex, for selected vorticities and assumed size and distribution of the vortex cores. Here we present the full evolution of the LDOS of quasiparticle excitations in a mesoscopic superconducting disk, during the multi-to-giant vortex transition as a function of the magnetic field, where at each step we recalculate the distribution of the superconducting order parameter. In Fig. 3, we plot the zero-energy density of states $N(E = 0, T)$ integrated over the sample as a function of the applied magnetic field, for the $L = 3$ vortex configuration. $N(E = 0, T)$ increases with applied magnetic field, as in the case of an isolated vortex [16]. When the giant vortex is assembled from the multivortex molecule, the LDOS profile changes from several individual peaks located at each vortex to a ringlike bound state with (without) an enclosed peak for odd (even) vorticity (as in Ref. [17]). Bound states are also found near the sample boundary, due to their lowered (nonzero) gap in the presence of strong circular Meissner currents. The representative contour plots of LDOS for $L = 3$ are shown in Fig. 3 as insets. As our main observation, we point out a clear drop of $N(E = 0)$ vs the magnetic field at the multi-to-giant vortex transition (see Fig. 3), where the LDOS

profile goes through a change of symmetry from a three-fold to a circular symmetric one. We thus confirm that the evolution of LDOS with magnetic field is directly linked to the specific heat and the thermal conductivity of the sample. To enforce this argument, the LDOS can be expressed as $N(E, T)/N_0 = N(E = 0, T) + \alpha_E |E|/\Delta_0$, and $N(E = 0, T)/N_0 = \gamma' + \alpha_k T/T_c$. Through the relation $C(T)/T = (2/T) \int_0^\infty dE[EN(E, T)\partial f(E, T)/\partial T]$, using the Fermi distribution function $f(E, T)$, one obtains $C(T)/(\gamma_n T) \sim N(E = 0, T)/N_0 + \alpha_E |E|/\Delta_0$ which unambiguously shows the link between the calculated curves in Figs. 2 and 3.

The jump of heat capacity between different vortex phases can also be expressed using other thermodynamic arguments. The discontinuity in the specific heat at a phase transition (at field H^*) can be calculated as [18]

$$C_i - C_j = -T\left(\frac{dH^*}{dT}\right)^2\left[\left(\frac{\partial M}{\partial H}\right)_i - \left(\frac{\partial M}{\partial H}\right)_j\right], \quad (4)$$

where M denotes sample magnetization. Here we apply the above expression to the multi-to-giant vortex transition, where i represents the vortex state of vorticity L just prior, and j represents the L vortex state just after the transition. Knowing the result for heat capacity vs H at the multi-to-giant vortex transition, we therefore expect to see similar features in the magnetic susceptibility $\chi = \partial M/\partial H$. We calculate the magnetization M as expelled magnetic field from the sample $\mathbf{M} = (\langle \mathbf{h} \rangle - \mathbf{H})/4\pi$, where $\langle \mathbf{h} \rangle$ is the local magnetic field averaged over the sample volume. The results of this calculation are shown in Fig. 4. They (i) confirm the link between (independently calculated) sharp changes in heat capacity and χ as a function of the
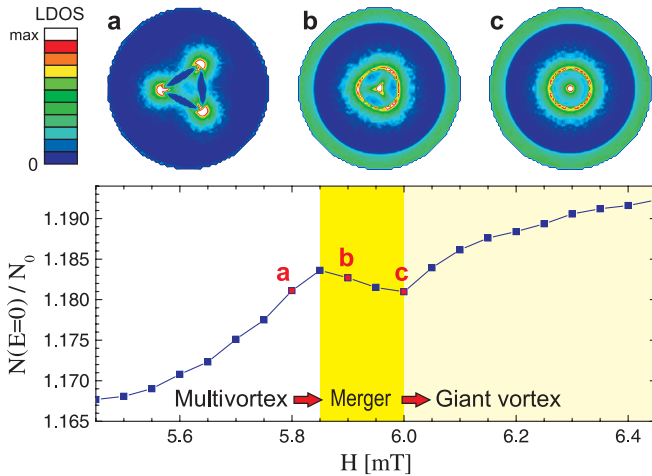

FIG. 3 (color online). The integrated zero-energy density of states (LDOS) as a function of the magnetic field for $L = 3$, for a superconducting disk with the same parameters as in Fig. 1. (a)–(c) are the representative contour plots of LDOS in the disk, at indicated magnetic fields. Interestingly, $N(0)[a] \approx N(0)[b] \approx N(0)[c]$.
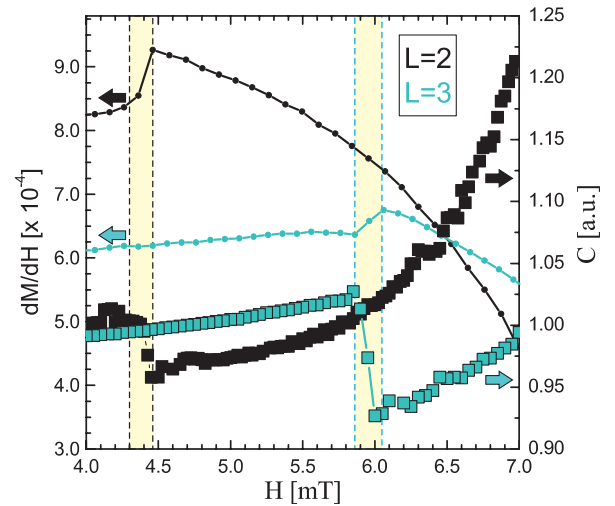

FIG. 4 (color online). The multi-to-giant vortex transition revealed through the sharp change in magnetic susceptibility as a function of applied magnetic field, showing direct correlations with the heat capacity, for states with vorticity 2 and 3. Shaded areas indicate the observed regions of giant-vortex formation in both quantities.
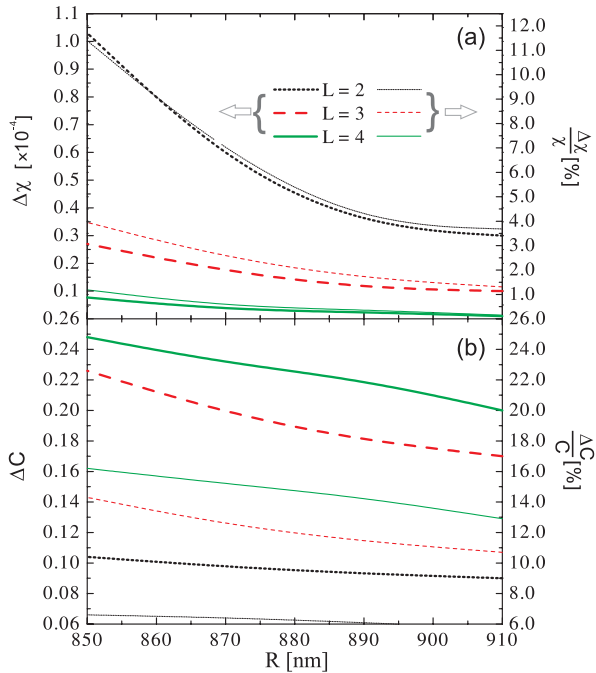
FIG. 5 (color online). The absolute and relative size of the jump at the multi-to-giant vortex transition, in (a) $\chi(H)$ curves, and (b) $C(H)$ curves, for vorticity $L = 2$, 3, and 4.

magnetic field, and (ii) show that assembly of a giant vortex in superconductors can be detected even by conventional magnetometry.

The above prediction is of immediate relevance to experiments, since both calorimetry and magnetometry are readily performed on mesoscopic superconductors. Of course, the question of sensitivity and resolution of the measurement is an open one, and we address this issue in Fig. 5. First, we determined the multi-to-giant vortex transition field H^* as a function of the size of the Al disk. For all considered vorticities ($L = 2 - 4$), H^* was found to increase with the radius of the sample. We then scanned the heat capacity and magnetic susceptibility versus applied field for every size of the sample, and recorded the size of the observed jump between values prior and after H^*. In Fig. 5 we show the absolute and relative size of the jump of both magnetic susceptibility (b) and heat capacity (c) at temperature 1.1 K. We found that the susceptibility shows a clearer signal at the multi-to-giant transition for lower vorticity, whereas corresponding discontinuity of heat capacity is more pronounced at higher vorticity. Note, however, that ΔC and $\Delta \chi$ should be directly proportional, according to Eq. (4). They indeed are, when susceptibility is calculated by $\chi = \partial^2 G / \partial H^2$, while we here used the experimental definition of magnetization as the flux expelled from the sample (which is directly measured by Hall magnetometry).

In summary, we demonstrated that second-order transitions between multi- and giant-vortex states in mesoscopic superconductors can be detected using calorimetry. The local density of states for quasiparticles in and around vortex cores changes when the vortex configuration changes, which affects the heating properties of the system. The observed sharp change in the heat capacity at the multi-to-giant vortex transition can also be linked to the magnetic susceptibility, enabling the observation of this transition by Hall magnetometry. Our results are therefore of immediate relevance to experimental efforts in the field, and further work is needed to generalize our findings to other systems, such as, e.g., Bose-Einstein condensates [1].

*francois.peeters@ua.ac.be
[1] D. A. Butts and D. S. Rokhsar, Nature (London) **397**, 327 (1999); A. E. Leanhardt et al., Phys. Rev. Lett. **89**, 190403 (2002).
[2] C. Reichhardt and C. J. Olson, Phys. Rev. Lett. **88**, 248301 (2002).
[3] M. Berciu, T. G. Rappoport, and B. Jankó, Nature (London) **435**, 71 (2005).
[4] C.-S. Lee et al., Nature (London) **400**, 337 (1999).
[5] V. A. Schweigert, F. M. Peeters, and P. S. Deo, Phys. Rev. Lett. **81**, 2783 (1998).
[6] I. V. Grigorieva et al., Phys. Rev. Lett. **99**, 147003 (2007).
[7] A. Kanda et al., Phys. Rev. Lett. **93**, 257002 (2004); M. V. Milošević et al., Phys. Rev. Lett. **103**, 217003 (2009).
[8] O. Bourgeois et al., Phys. Rev. Lett. **94**, 057007 (2005).
[9] A. K. Geim et al., Nature (London) **390**, 259 (1997).
[10] M. V. Milošević and R. Geurts, Physica (Amsterdam) **470C**, 791 (2010).
[11] P. S. Deo, J. P. Pekola, and M. Manninen, Europhys. Lett. **50**, 649 (2000).
[12] D. S. Golubović et al., Phys. Rev. B **71**, 180502 (2005) and references therein.
[13] F. Ong and O. Bourgeois, Europhys. Lett. **79**, 67003 (2007).
[14] C. Caroli, P. G. de Gennes, and J. Matricon, Phys. Lett. **9**, 307 (1964).
[15] N. Schopohl and K. Maki, Phys. Rev. B **52**, 490 (1995).
[16] M. Ichioka et al., Phys. Rev. B **53**, 15 316 (1996).
[17] A. S. Mel'nikov and V. M. Vinokur, Nature (London) **415**, 60 (2002); Phys. Rev. B **65**, 224514 (2002).
[18] P. G. de Gennes, Superconductivity of Metals and Alloys (Addison-Wesley, New York, 1994).